A Cu(II)-Mediated C−H Oxygenation of Sterically Hindered Tripyridine Ligands To Form Triangular $Cu(II)_3$ Complexes

Masahito Kodera,*,† Yoshimitsu Tachi,† Toshio Kita,† Hiromu Kobushi,† Yoshinori Sumi,† Koji Kano,† Motoo Shiro,‡ Masayuki Koikawa,§ Tadashi Tokii,§ Masaaki Ohba,|| and Hisashi Okawa||

Department of Molecular Science and Technology, Doshisha University, Kyotanabe, Kyoto 610-0321, Japan, X-ray Laboratory, Rigaku-Denki, Akishima, Tokyo 196, Japan, Department of Chemistry, Saga University, Saga 840, Japan, and Department of Chemistry, Kyushu University, Hakozaki, Higashi-ku, Fukuoka 812, Japan

Received March 24, 1999

Two sterically hindered tris-pyridyl methane ligands, tris(6-methyl-2-pyridyl)methane (L1) and bis(6-methyl-2-pyridyl)pyridylmethane (L2), are newly synthesized. Under aerobic conditions, L*n* ($n = 1$ or 2) reacts with CuX_2 (X = Cl or Br), oxygenated at the methine position to LnOH or LnOMe. The former alcoholate ligand creates trinuclear Cu(II) complexes $[Cu_3(X)(LnO)_3](PF_6)_2$ {(X, *n*) = (Br, 1) **1**, (Cl, 1) **2**, (Br, 2) **3**, or (Cl, 2) **4**} in which the alkoxide oxygen atoms bridge copper centers. The crystal structures of **1**−**4** are presented along with their magnetic susceptibility data. The weak antiferromagnetic coupling between the Cu(II) centers in this trinuclear arrangement is due to weak interaction of the magnetic orbitals (dz^2) which are oriented along three alternate sides in a hexagon of the Cu_3O_3 core in **1**−**4**. Under anaerobic conditions, L1 reacts with $CuBr_2$ to form a square pyramidal complex $[CuL1Br_2]$ (**9**) with the ligand facially capping. $[Cu(Br)_2(L1OMe)]$ (**10**) was obtained after the suspension of **9** in MeOH was stirred under air for 48 h. In the presence of cyclohexene, **9** is converted to $[Cu(Br)(L1)]_m$ ($m = 1$ or 2) **5** quantitatively to give *trans*-1,2-dibromocyclohexane, indicating that Br_2 is generated during the reaction. The FAB MS spectrum of $[^{18}O]$-**1** prepared by the reaction of L1 with $CuBr_2$ under $^{18}O_2$ shows that the ligand of $[^{18}O]$-**1** is $L1^{18}O^-$. $L1^{18}OH$, $L1OCD_3$, and bis(6-methyl-2-pyridyl) ketone were obtained from reaction of L1 with $CuBr_2$ in CD_3OD under $^{18}O_2$. These results indicate that the origins of the O atom in L1OH and L1OMe are O_2 and MeOH, respectively. On the basis of these results, a mechanism of the oxygenation of L1 in the present system will be proposed.

Introduction

Sterically hindered tridentate end-capping ligands, such as derivatives of hydrotrispyrazolylborate,[1] trisimidazolylphosphine,[2] and triazacyclononane,[3] are known to stabilize biologically relevant metal complexes and have led to great progress in understanding the structures and functions of non-heme metalloproteins.[4] μ-η^2:η^2-Peroxodicopper(II) complexes[5,6] of sterically hindered hydrotrispyrazolylborate ligands were used to exactly predict the Cu_2O_2 structure of oxyhemocyanine before the structure of oxyhemocyanine was determined by X-ray analysis.[7] It is reported that the μ-η^2:η^2-peroxodicopper(II) complex is also stabilized by sterically hindered trisimidazolylphosphine ligands.[2] As a similar ligand, trispyridylmethane is known to stabilize low valence state of various metal ions[8−13] and is more easily prepared than the pyrazolyl and imidazol derivatives.[14−17] However, few examples of sterically hindered derivatives of the trispyridylmethane ligand have been known.[18,19] Here, we prepared the sterically hindered trispyridylmethane ligands tris(6-methyl-2-pyridyl)methane (L1) and bis(6-methyl-2-pyridyl)pyridylmethane (L2). On the contrary, to the expectation that L1 and L2 would form di-μ-hydroxodicopper(II) complexes upon reaction with CuX_2 (X = Br and Cl) and

* To whom correspondence should be addressed. Telephone number: +81-774-65-6652. Fax number: +81-774-65-6848. E-mail address: mkodera@mail.doshisha.ac.jp.

† Doshisha University.

‡ Rigaku-Denki.

§ Saga University.

|| Kyushu University.

(1) Kitajima, N.; Moro-oka, Y. *Chem. Rev.* **1994**, *94*, 737.
(2) Sorrell, T. N.; Allen, W. E.; White, P. S. *Inorg. Chem.* **1995**, *34*, 952.
(3) Mahapatra, S.; Halfen, J. A.; Wilkinson, E. C.; Pan, G.; Wang, X.; Young, V. G., Jr.; Cramer, C. J.; Que, L., Jr.; Tolman, W. B. *J. Am. Chem. Soc.* **1996**, *118*, 11555.
(4) Holm, R. H.; Solomon, E. I. *Chem. Rev.* **1996**, *96*, 2237.
(5) Kitajima, N.; Fukui, H.; Moro-oka, Y. *Chem. Commun.* **1988**, 485.
(6) Kitajima, J.; Fujisawa, K.; Moro-oka, Y.; Toriumi, K. *J. Am. Chem. Soc.* **1989**, *111*, 8975.
(7) Magnus, K.; Ton-That, H. *J. Inorg. Biochem.* **1992**, *47*, 20.
(8) Canty, A. J.; Chaichit, N.; Gatehouse, B. M.; George, E. E.; Hayhurst, G. *Inorg. Chem.* **1981**, *20*, 2414.
(9) Canty, A. J.; Chaichit, N.; Gatehouse, B. M.; George, E. E. *Inorg. Chem.* **1981**, *20*, 4293.
(10) Canty, A. J.; Minchin, N.; Healy, P. C.; White, A. H. *J. Chem. Soc., Dalton Trans.* **1982**, 1795.
(11) Canty, A. J.; Patrick, J. M.; White, A. H. *Inorg. Chem.* **1984**, *23*, 3827.
(12) Szalda, D. J.; Keene, F. R. *Inorg. Chem.* **1986**, *25*, 2795.
(13) Keene, F. R.; Szalda, D. J.; Wilson, T. A. *Inorg. Chem.* **1987**, *26*, 2211.
(14) Tang, C. C.; Davalian, D.; Huang, P.; Breslow, R. *J. Am. Chem. Soc.* **1978**, *100*, 3918.
(15) Mani, F. *Coord. Chem. Rev.* **1992**, *120*, 325.
(16) White, D. L.; Faller, J. W. *Inorg. Chem.* **1982**, *21*, 3119.
(17) Keene, F. R.; Snow, M. R.; Stephenson, P. J.; Tiekink, E. R. T. *Inorg. Chem.* **1988**, *27*, 2040.
(18) Kodera, M.; Shimakoshi, H.; Nishimura, M.; Okawa, H.; Iijima, S.; Kano, K. *Inorg. Chem.* **1996**, *35*, 4967.
(19) Jonas, R. T.; Stack, T. D. P. *Inorg. Chem.* **1998**, *37*, 6615.

10.1021/ic990331g CCC: $19.00
Published on Web 12/23/1999

NaOH, equilateral triangular $Cu(II)_3$ complexes $[Cu_3(X)(LnO)_3](PF_6)_2$ {(X, n) = (Br, 1) **1**; (Cl, 1) **2**; (Br, 2) **3**, and (Cl, 2) **4**} were obtained. In the reaction, L*n* is oxygenated at the methine position to LnO^-.

Many examples of equilateral triangular Cu_3 complexes have been reported.[20−32] Most of them have one or two μ_3-hydroxo (or μ_3-oxo) bridges and show strong antiferromagnetic interaction between the three Cu(II) ions.[20−32] The structures and magnetic properties of **1**−**4** are quite unique because the μ_3-bridges in **1**−**4** are a Br or a Cl ion, which is easily removed, and a very weak antiferromagnetic interaction operates among the three Cu(II) ions in **1**−**4**. Therefore, it might be important to clarify the reason for the weak antiferromagnetic interaction in **1**−**4** on the basis of their crystal structures.

Oxygenation of C−H groups catalyzed by metal ions has attracted the interest of chemists because of the importance in synthetic chemistry[33] and in model studies of non-heme-monooxygenases.[33−38] The oxygenation of aromatic[39−42] and aliphatic[43−45] C−H groups of ligands via Cu(I)-mediated O_2-activation as models of copper-containing monooxygenases has been reported, where O_2 is bound to the dicopper(I) center and activated to a highly electrophilic species[42] to oxygenate the aromatic C−H and to a di-μ-oxodicopper(III) complex[43−46] for the aliphatic one. A ligand ketonization is known as a different type of ligand oxygenation, in which methylene groups substituted by two imines or aromatic amines are ketonized under air in the presence of metal ions, such as Cu(I), Cu(II), Fe(II), Fe(III), Co(II), and Co(III).[47−53] The Cu(II)-mediated ketonization of diiminomethane,[50] dibenzoimidazolylmethane,[48] dipyridylmethane,[53] and their derivatives has been reported. The mechanism of the ketonization seems to be a kind of autoxidation via an alkylhydroperoxide intermediate.[50,51] As a similar oxidation of ligands, imidation of α-aminomalonate catalyzed by a Co(III) ion is known.[54,55] Although the ketonization is not biologically relevant, the reactions are synthetically promising because most of them are catalytic and quantitative. This type of reaction, however, has never been successfully applied to hydroxylation of a C−H group of a ligand.

In this study, we describe the synthesis of L*n* (n = 1 and 2) and the crystal structures and magnetic properties of **1**−**4** and propose a mechanism of the hydroxylation of L1 in the reaction with $CuBr_2$ in MeOH under air.

Experimental Section

All ordinary reagents and solvents were purchased and used as received unless otherwise noted. Tetrahydrofuran (THF) was dried over sodium metal and distilled. Absolute MeOH was obtained by distillation over Mg. MeCN and CH_2Cl_2 were dried over P_2O_5 and distilled.

Measurements. Elemental analyses (C, H, and N) were carried out at the Elemental Analysis Service Center of Kyoto University. The amounts of copper were analyzed on a Shimazu AA-610 atomic absorption/flame emission spectrophotometer. UV−vis absorption spectra were recorded on a Hitachi U-3210 spectrophotometer and on a Shimadzu UV-3100 spectrophotometer in MeCN. Infrared (IR) spectra were taken on a Shimadzu IR-400 spectrometer with KBr disks. Fast atom bombardment (FAB) mass spectra were obtained on a JEOL JMS-DX 300 spectrometer using *m*-nitrobenzyl alcohol (NBA) as a matrix. ^{1}H NMR spectra in $CDCl_3$ were recorded on a JEOL JMN-A 400 spectrometer by using Me_4Si as an internal standard. EPR spectra were recorded on a JEOL JES-TE 200 spectrometer in MeCN at 4.2−77 K. Magnetic susceptibilities were measured by the use of a HOXAN HSM-D SQUID susceptometer in the temperature range of 4.2−100 K (applied magnetic field of 100 G) and by the use of a Faraday balance in the temperature range 80−290 K (applied magnetic field of 3000 G). Calibrations were made with $Mn(NH_4)_2(SO_4)_2\cdot 6H_2O$ for the SQUID susceptometer and with $[Ni(en)_3][S_2O_3]$ for the Faraday balance. Diamagnetic corrections were made with Pascal's constants.[56] Effective magnetic moments were calculated by the equation $\mu_{eff} = 2.828(\chi_M T)^{1/2}$, where χ_M is the molar magnetic susceptibility corrected for diamagnetism of the constituent atoms. GLC analysis of 1,2-dibromocyclohexane was carried out by using a Shimadzu GC-8A gas chromatograph using a thermon-1000 + H_3PO_4 column (3 mm diameter × 0.8 m, at gradient temperature 80−240 °C for 20 min, He carrier 0.5 kg/cm^2).

Preparations. Bis(6-methyl-2-pyridyl)methane. In dry THF (100 mL) was dissolved 2,6-lutidine (10.7 g, 0.1 mol) and the solution was degassed by evacuation and refilling with Ar. To the solution was added

(20) Chakravorty, A.; Baral, S. *Inorg. Chim. Acta* **1980**, *39*, 1.
(21) Datta, D.; Masharak, P. K.; Chakravorty, A. *Inorg. Chem.* **1981**, *20*, 1673.
(22) Datta, D.; Chakravorty, A. *Indian J. Chem.* **1981**, *20A*, 1101.
(23) Datta, D.; Chakravorty, A. *Inorg. Chem.* **1982**, *21*, 363.
(24) Datta, D.; Chakravorty, A. *Inorg. Chem.* **1983**, *22*, 1611.
(25) Butcher, R. J.; O'Connor, C. J.; Sinn, E. *Inorg. Chem.* **1981**, *20*, 537.
(26) Mohan, M.; Kumar, M. *Transition Met. Chem.* **1982**, *7*, 301.
(27) Hulsbergen, F. B.; Hoedt, R. W. M.; Verschoor, G. C.; Reedijk, J.; Spek, A. L. *J. Chem. Soc., Dalton Trans.* **1983**, 539.
(28) Costes, J. P.; Dahan, F.; Laurent, J. P. *Inorg. Chem.* **1986**, *25*, 413.
(29) Kwiatkowski, M.; Kwiatkowski, E.; Olechinowicz, A.; Ho, D. M.; Deutsch, E. *Inorg. Chim. Acta* **1988**, *150*, 65.
(30) Agnus, Y.; Metz, L. B.; Boudon, C.; Gisselbrecht, J. P.; Gross, M. *Inorg. Chem.* **1991**, *30*, 3155.
(31) Comarmond, J.; Dietrich, B.; Lehn, J.-M.; Louis, R. *J. Chem. Soc., Chem. Commun.* **1985**, 74.
(32) Cole, A. P.; Root, D. E.; Mukherjee, P.; Solomon, E. I.; Stack, T. D. P. *Science* **1996**, *273*, 1848.
(33) Hill, C. L. In *Activation and Functionalization of Alkanes*; Hill, C. L., Ed.; John Wiley & Sons: New York, 1989; p 243.
(34) Klinman, J. P.; Berry, J. A.; Tian, G. In *Bioinorganic Chemistry of Copper*; Karlin, K. D.; Tyeklár, Z., Ed.; Chapman & Hall: New York, 1993; p 151.
(35) Blackburn, N. J. In *Bioinorganic Chemistry of Copper*; Karlin, K. D., Tyeklár, Z., Ed.; Chapman & Hall: New York, 1993; p 164.
(36) Chan, S. I.; Nguyen, H.-H. T.; Shiemke, A. K.; Lindstrom, M. E. In *Bioinorganic Chemistry of Copper*; Karlin, K. D., Tyeklár, Z., Ed.; Chapman & Hall: New York, 1993; p 184.
(37) Merkler, D. J.; Kulathila, R.; Young, S. D.; Freeman, J.; Villafranca, J. J. In *Bioinorganic Chemistry of Copper*; Karlin, K. D., Tyeklár, Z., Ed.; Chapman & Hall: New York, 1993; p 196.
(38) Kodera, M.; Kano, K.; Funabiki, T. In *Oxygenases and Model Systems*; Funabiki, T., Ed.; Kluwer Academic Publishers: Dordrecht, 1997; Vol. 19, p 283.
(39) Karlin, K. D.; Hayes, J. C.; Gultneh, Y.; Cruse, R. W.; McKown, J. W.; Hutchinson, J. P.; Zubieta, J. *J. Am. Chem. Soc.* **1984**, *106*, 2121.
(40) Karlin, K. D.; Cohen, B. I.; Jacobson, R. R.; Zubieta, J. *J. Am. Chem. Soc.* **1987**, *109*, 6194.
(41) Karlin, K. D.; Nasir, M. S.; Cohen, B. I.; Cruse, R. W.; Kaderli, S.; Zuberbüler, A. D. *J. Am. Chem. Soc.* **1994**, *116*, 1324.
(42) Pidcock, E.; Obias, H. V.; Zhang, C. X.; Karlin, K. D.; Solomon, E. I. *J. Am. Chem. Soc.* **1998**, *120*, 7841.
(43) Mahapatra, S.; Halfen, J. A.; Wilkinson, E. C.; Que, L., Jr.; Tolman, W. B. *J. Am. Chem. Soc.* **1994**, *116*, 9785.
(44) Itoh, S.; Kondo, T.; Komatsu, M.; Ohshiro, Y.; C. Li; Kanehisa, N.; Y. Kai; Fukuzumi, S. *J. Am. Chem. Soc.* **1995**, *116*, 4717.
(45) Itoh, S.; Nakao, H.; Berreau, L. M.; Kondo, T.; Komatsu, M.; Fukuzumi, S. *J. Am. Chem. Soc.* **1998**, *120*, 2890.
(46) Halfen, J. A.; Mahapatra, S.; Wilkinson, E. C.; Kaderli, S.; Young, V. G., Jr.; Que, L., Jr.; Zuberbüler, A. D.; Tolman, W. B. *Science* **1996**, *271*, 1397.
(47) Weiss, M. C.; Goedken, V. L. *J. Am. Chem. Soc.* **1976**, *98*, 3389.
(48) Sprecher, C. A.; Zuberbüler, A. D. *Angew. Chem., Int. Ed. Engl.* **1977**, *16*, 189.
(49) Durham, B.; Anderson, T. J.; Switzer, J. A.; Endicott, J. F.; Glick, M. D. *Inorg. Chem.* **1977**, *16*, 271.
(50) Urbach, F. L.; Knopp, U.; Zuberbüler, A. D. *Helv. Chim. Acta* **1978**, *61*, 1097.
(51) Switzer, J. A.; Endicott, J. F. *J. Am. Chem. Soc.* **1980**, *102*, 1181.
(52) Guillot, G.; Mulliez, E.; Leduc, P.; Chottard, J.-C. *Inorg. Chem.*, **1990**, *29*, 577.
(53) Lee, D.-H.; Murthy, N. N.; Karlin, K. D. *Inorg. Chem.* **1996**, *35*, 804.
(54) Yashiro, M.; Shimada, A.; Usui, T.; Yano, S.; Kobayashi, K.; Sakurai, T.; Yoshikawa, S. *J. Am. Chem. Soc.* **1985**, *107*, 4351.
(55) Kojima, T.; Hidai, M.; Kuroda, R.; Yano, S. *J. Am. Chem. Soc.* **1990**, *112*, 4576.
(56) Boudreaux, E. A.; Mulay, L. N. *Theory and Applications of Molecular Paramagnetism*; John Wiley & Sons Inc: New York, 1976.

n-butyllithium [(1.69 M in hexane), 125 mL, 0.21 mol] at −78 °C. The solution was warmed to room temperature and stirred for 3 h under Ar. The solution was cooled to −78 °C and a suspension of anhydrous $ZnCl_2$ (30 g, 0.22 mol) in dry THF (100 mL) was added. The mixture was warmed to room temperature and stirred for 1 h under Ar. To the mixture were added Pd(dppf)Cl_2 (0.73 g, 0.001 mol) and 2-bromo-6-picoline (18.9 g, 0.11 mol) at −78 °C. The mixture was warmed to room temperature and heated to reflux with vigorous stirring for 15 h under Ar. After the resultant mixture was cooled to room temperature, THF was removed by distillation. The residue was suspended in $CHCl_3$ (100 mL). To the suspension were added an aqueous solution (10 mL) of NaOH (4.4 g, 0.11 mol) and a saturated aqueous solution of $Na_2S\cdot 9H_2O$ (26.4 g, 0.11 mol), and the mixture stirred for 1 h to give a white precipitate. The precipitate was removed by filtration and washed with $CHCl_3$ (200 mL). The filtrate and washings were transferred to a separatory funnel, and the $CHCl_3$ layer was separated. The aqueous layer was extracted with $CHCl_3$ (80 mL × 5). The $CHCl_3$ layers were combined and dried over anhydrous Na_2SO_4 and concentrated to dryness. The oily residue was purified by vacuum distillation (0.1 Torr, 80−120 °C). Bis(6-methyl-2-pyridyl)methane (13.3 g, yield 67%) was obtained. IR data [ν/cm^{-1}]: 3050 (pyridine C−H), 2900 (aliphatic C−H), 1590, 1570 (pyridine ring), 1450 (C−H bending), 830, 790, and 770 (pyridine C−H bending). ^{1}H NMR data (δ/ppm vs Me_4Si in $CDCl_3$): 7.47 (t, 2H, py-4), 6.99 (d, 4H, py-3, 5), 4.29 (s, 2H, $-CH_2-$), and 2.55 (s, 6H, CH_3). FAB-MS data: *m*/*z* 198 [M]$^+$, 106 [M − Mepy]$^+$.

Tris(6-methyl-2-pyridyl)methane (L1). In dry THF (100 mL) was dissolved bis(6-methyl-2-pyridyl)methane (9.91 g, 0.05 mol) and the solution was degassed by evacuation and refilling with Ar. To the solution was added *n*-BuLi [(1.64 M in hexane), 33.5 mL, 0.055 mol] at −78 °C. The solution was warmed to room temperature and stirred for 3 h under Ar. To the solution were added Pd(PPh_3)$_4$ (0.58 g, 0.0005 mol) and 2-bromo-6-picoline (9.46 g, 0.055 mol) at −78 °C. The mixture was warmed to room temperature and heated to reflux with vigorous stirring for 15 h under Ar. The reaction mixture was cooled to room temperature and concentrated to dryness. To the residue were added H_2O (100 mL) and $CHCl_3$ (200 mL). The $CHCl_3$ layer was separated by a separatory funnel and the aqueous layer was extracted with $CHCl_3$ (150 mL × 4). The $CHCl_3$ layers were combined and dried with anhydrous Na_2SO_4 and concentrated to dryness. Upon addition of Et_2O to the residue, a white solid precipitated. The solid was collected by filtration and washed with Et_2O several times. L1 (8.22 g, yield 57%) was obtained. Anal. Calcd for $C_{19}H_{19}N_3$: C, 78.86; H, 6.62; N, 14.52. Found: C, 78.57; H, 6.52; N, 14.22. IR data [ν/cm^{-1}] on KBr disk: 3050 (pyridine C−H), 2950, 2900 (aliphatic C−H), 1600, 1580, 1565 (pyridine ring), 1450 (C−H bending), 840, and 775 (pyridine C−H bending). ^{1}H NMR data (δ/ppm vs Me_4Si in $CDCl_3$): 7.47 (t, 3H, py-4), 7.04 (d, 3H, py-3), 6.99 (t, 3H, py-5), 5.90 (s, 1H, methine), and 2.50 (s, 9H, methyl). FAB-MS data: *m*/*z* 289 [M]$^+$ 197 [M − Mepy]$^+$.

Bis(6-methyl-2-pyridyl)(2-pyridyl)methane (L2). L2 (yield 68%) was synthesized by the same method as L1 using 2-bromopyridine in place of 2-bromo-6-picoline. Anal. Calcd for $C_{19}H_{19}N_3$: C, 78.52; H, 6.22; N, 15.26. Found: C, 78.22; H, 6.28; N, 14.96. IR data [ν/cm^{-1}] on KBr disk: 3050 (pyridine C−H), 2900 (aliphatic C−H), 1585, 1565 (pyridine ring), 1470, 1450, 1425 (C−H bending), 820, 775, and 750 (pyridine C−H bending). ^{1}H NMR data (δ/ppm vs Me_4Si in $CDCl_3$): 8.75 (dq, 1H, py-6), 7.60, (dt, 1H, py-4), 7.49 (t, 2H, Mepy-4), 7.25 (t, 1H, py-3), 7.12 (t, 1H, py-5), 7.09 (dd, 2H, Mepy-3), 6.99 (dd, 2H, py-5), 5.93 (s, 1H, methine), and 2.51 (s, 6H, methyl). FAB-MS data: *m*/*z* 276 [M]$^+$, 197 [M − py]$^+$, 183 [M − Mepy]$^+$.

[Cu_3(Br)(L1O)$_3$](PF_6)$_2\cdot C_6H_6$ (1$\cdot C_6H_6$). Stoichiometric Reaction. To a solution of $CuBr_2$ (223 mg, 1.0 mmol) in MeOH (10 mL) was added a solution of L1 (289 mg, 1 mmol) in MeOH (5 mL) with stirring, then a brown solid precipitated immediately. Stirring was continued for 24 h under air. To the resultant brown suspension was added a solution of NaOH (50 mg, 1.25 mmol) in MeOH (5 mL). The mixture was stirred at room temperature for 18 h, and the brown suspension turned green with a yellow precipitate. The yellow precipitate was collected by filtration and was characterized to be the Cu(I) bromide complex of L1 [Cu(Br)(L1)]$_m$ (m = 1 or 2), **5** (207 mg, yield 48%). To the filtrate was added NH_4PF_6 (200 mg, 1.23 mmol), and the tricopper(II) bromide complex of L1O (**1**) precipitated as green solid, which was collected by filtration (182 mg, yield 37%). The powder of **1** was recrystallized from MeCN/CH_2Cl_2/C_6H_6 to give crystals (**1**$\cdot C_6H_6$) suitable for X-ray structure analysis. **1**$\cdot C_6H_6$: Anal. Calcd for $C_{63}H_{60}N_9O_3P_2F_{12}Cu_3Br$: C, 48.11; H, 3.90; N, 8.12; Cu, 12.29. Found: C, 49.17; H, 3.98; N, 8.39; Cu, 11.90. UV−vis absorption data (in MeCN) [λ_{max}/nm (ϵ_{max}/dm^3 mol^{-1} cm^{-1})]: 270 (52 600) and 770 (530). IR data [ν/cm^{-1}] on KBr disk: 3050 (aromatic C−H), 2900 (aliphatic C−H), 1600, 1580, 1565 (pyridine ring), 1450 (C−H bending), 1085 (C−O), 840 (PF_6), and 785 (pyridine C−H bending). FAB-MS data: *m*/*z* 1325 [M]$^+$, 1246 [M − Br]$^+$, 1180 [M − PF_6]$^+$, and 1101 [M − Br − PF_6]$^+$. **5**: Anal. Calcd for $C_{19}H_{19}N_3CuBr$: C, 52.90; H, 4.44; N, 9.75. Found: C, 52.23; H, 4.39; N, 9.48. UV−vis absorption data (in MeCN) [λ_{max}/nm (ϵ_{max}/dm^3 mol^{-1} cm^{-1})]: 254 (15 000), 268 (15 000), and 333 (2500). IR data [ν/cm^{-1}] on KBr disk: 3050 (aromatic C−H), 2950, 2900 (aliphatic C−H), 1590, 1570, 1560 (pyridine ring), 1450 (C−H bending), and 780 (pyridine C−H bending). FAB-MS data: *m*/*z* 433 [M]$^+$, 352 [M − Br]$^+$.

Catalytic Reaction. A mixture of $CuBr_2$ (22.3 mg, 0.1 mmol) and L1 (289 mg, 1 mmol) in MeOH (15 mL) was stirred for 24 h to produce a green solution. To the solution were added $CuBr_2$ (200.7 mg, 0.9 mmol) and NaOH (50 mg, 1.25 mmol). Stirring was further continued for 18 h. NH_4PF_6 (200 mg, 1.23 mmol) was added to the reaction mixture, and **1** (312 mg, yield 64%) was obtained as green powder. The Cu(I) complex **5** was not obtained in the catalytic reaction. The yield of **1** was increased to 67% when $CuBr_2$ and NaOH were added to the resultant mixture after the reaction of L1 with the catalytic amount of $CuBr_2$ was continued for 2 days.

[Cu_3(Cl)(L1O)$_3$](PF_6)$_2\cdot$MeCN$\cdot CH_2Cl_2\cdot C_6H_6$ (2$\cdot$MeCN$\cdot CH_2Cl_2\cdot C_6H_6$). The tricopper(II) chloride complex of L1O (**2**) (yield 35%) was obtained as a bluish green powder by the reaction of L1 with $CuCl_2$ under the stoichiometric conditions shown in the synthesis of **1**. The Cu(I) chloride complex of L1 [Cu(Cl)(L1)]$_m$ (m = 1 or 2) (**6**) (yield 15%) was isolated as yellow powder. The powder of **2** was recrystallized from MeCN/CH_2Cl_2/C_6H_6 to give crystals (**2**$\cdot$MeCN$\cdot CH_2Cl_2\cdot C_6H_6$) suitable for X-ray structure analysis. **2**$\cdot$MeCN$\cdot CH_2Cl_2\cdot C_6H_6$: Anal. Calcd for $C_{66}H_{65}N_{10}O_3P_2F_{12}Cu_3Cl_3$: C, 48.54; H, 4.01; N, 8.39; Cu, 11.90. Found: C, 48.52; H, 4.01; N, 8.52; Cu, 11.90. UV−vis absorption data (in MeCN) [λ_{max}/nm (ϵ_{max}/dm^3 mol^{-1} cm^{-1})]: 270 (63 000) and 771 (515). IR data [ν/cm^{-1}] on KBr disk: 3050 (aromatic C−H), 2900 (aliphatic C−H), 1600, 1580, 1565 (pyridine ring), 1450 (C−H bending), 1090 (C−O), 840 (PF_6), and 785 (pyridine C−H bending). FAB-MS data: *m*/*z* 1281 [M]$^+$, 1246 [M − Cl]$^+$, 1136 [M − PF_6]$^+$, and 1101 [M − Cl − PF_6]$^+$. **6**: Anal. Calcd for $C_{19}H_{19}N_3$-CuCl: C, 58.91; H, 4.95; N, 10.85. Found: C, 58.15; H, 4.76; N, 10.59. UV−vis absorption data (in MeCN) [λ_{max}/nm (ϵ_{max}/dm^3 mol^{-1} cm^{-1})]: 254 (15 000), 268 (15 000), and 333 (2500). IR data [ν/cm^{-1}] on KBr disk: 3050 (aromatic C−H), 2950, 2900 (aliphatic C−H), 1590, 1570, 1560 (pyridine ring), 1450 (C−H bending), and 780 (pyridine C−H bending). FAB-MS data: *m*/*z* 387 [M]$^+$, 352 [M − Cl]$^+$.

[Cu_3(Br)(L2O)$_3$](PF_6)$_2$ (3). The tricopper(II) bromide complex of L2O (**3**) (yield 44%) was obtained as green powder by the reaction of L2 with $CuBr_2$ under the stoichiometric conditions shown above. The Cu(I) bromide complex of L2 [Cu(Br)(L2)]$_m$ (m = 1 or 2), **7**, did not precipitate during the reaction. **7** (170 mg, yield 41%) was obtained as yellow powder by concentration of the filtrate. The powder of **3** was recrystallied from MeCN/CH_2Cl_2/C_6H_6 to give crystals (**3**) suitable for X-ray structure analysis. **3**: Anal. Calcd for $C_{54}H_{48}N_9O_3P_2F_{12}Cu_3Br$: C, 45.31; H, 3.38; N, 8.81; Cu, 13.32. Found: C, 44.89; H, 3.43; N, 8.84; Cu, 12.93. UV−vis absorption data (in MeCN) [λ_{max}/nm (ϵ_{max}/dm^3 mol^{-1} cm^{-1})]: 266 (51 700) and 757 (507). IR data [ν/cm^{-1}] on KBr disk: 3050 (aromatic C−H), 2900 (aliphatic C−H), 1600, 1580, 1565 (pyridine ring), 1460, 1445 (C−H bending), 1090 (C−O), 840 (PF_6), and 800, 775 (pyridine C−H bending). FAB-MS data: *m*/*z* 1283 [M]$^+$, 1204 [M − Br]$^+$, 1138 [M − PF_6]$^+$, and 1059 [M − Br − PF_6]$^+$. **7**: Anal. Calcd for $C_{18}H_{17}N_3CuBr$: C, 51.80; H, 4.11; N, 10.07. Found: C, 51.19; H, 4.09; N, 9.89. UV−vis absorption data (in MeCN) [λ_{max}/nm (ϵ_{max}/dm^3 mol^{-1} cm^{-1})]: 256 (12 900), 264 (13 400), and 323 (1800). IR data [ν/cm^{-1}] on KBr disk: 3050 (aromatic C−H), 2950, 2900 (aliphatic C−H), and 1590, 1570, 1560 (pyridine ring), 1460,

1450, 1430 (C−H bending), and 770 (pyridine C−H bending). FAB-MS data: *m*/*z* 419 $[M]^+$, 338 $[M - Br]^+$.

$[Cu_3(Cl)(L2O)_3](PF_6)_2 \cdot C_6H_6$ ($4 \cdot C_6H_6$). The tricopper(II) chloride complex of L2O (**4**) (yield 39%) was obtained as bluish green powder by the reaction of L2 with $CuCl_2$ under the stoichiometric conditions shown above. The Cu(I) chloride complex $[Cu(Cl)L2]_m$ ($m = 1$ or 2), **8**, was not isolated but detected by a IR spectrum of a crude residue obtained by concentration of the filtrate after **4** was isolated by filtration. **8** was synthesized by a reaction of L2 with CuCl to confirm the formation of **8** on the reaction of L2 with $CuCl_2$. The powder of **4** was recrystallized from $MeCN/CH_2Cl_2/C_6H_6$ to give crystals ($4 \cdot C_6H_6$) suitable for X-ray structure analysis. $4 \cdot C_6H_6$: Anal. Calcd for $C_{60}H_{54}N_9O_3P_2F_{12}Cu_3Cl$: C, 49.19; H, 3.71; N, 8.60; Cu, 13.01. Found: C, 48.97; H, 3.83; N, 8.57; Cu, 12.93. UV−vis absorption data (in MeCN) [λ_{max}/nm (ϵ_{max}/dm^3 mol^{-1} cm^{-1})]: 266 (53 700) and 752 (456). IR data [ν/cm^{-1}] on KBr disk: 3050 (aromatic C−H), 2950 (aliphatic C−H), 1600, 1585 (pyridine ring), 1460, 1450, (C−H bending), 1090 (C−O), 840 (PF_6), and 880, 775 (pyridine C−H bending). FAB-MS data: *m*/*z* 1239 $[M]^+$, 1204 $[M - Cl]^+$, 1094 $[M - PF_6]^+$, and 1059 $[M - Cl - PF_6]^+$. **8**: Anal. Calcd for $C_{18}H_{17}N_3CuCl$: C, 57.90; H, 4.59; N, 11.26. Found: C, 56.33; H, 4.39; N, 10.54. UV−vis absorption data (in MeCN) [λ_{max}/nm (ϵ_{max}/dm^3 mol^{-1} cm^{-1})]: 254 (14 000), 263 (14 000), and 324 (2100). IR data [ν/cm^{-1}] on KBr disk: 3050 (aromatic C−H), 2950, 2900 (aliphatic C−H), 1590, 1570 1560 (pyridine ring), 1460, 1450, 1430 (C−H bending), and 765 (pyridine C−H bending). FAB-MS data: *m*/*z* 373 $[M]^+$, 338 $[M - Cl]^+$.

$[Cu(Br)_2(L1)]$ (9). To a solution of $CuBr_2$ (223 mg, 1.0 mmol) in MeOH (5 mL) was added a solution of L1 (289 mg, 1.0 mmol) in MeOH (5 mL) with stirring, then **9** (yield 90%) precipitated immediately as brown solid. The brown solid of **9** was recrystallized from $CH_2Cl_2/C_6H_6/Et_2O$ under Ar to give crystals suitable for X-ray structure analysis. **9**: Anal. Calcd for $C_{19}H_{19}N_3CuBr_2$: C, 44.51; H, 3.74; N, 8.20; Cu, 12.39. Found: C, 44.23; H, 3.76; N, 8.12; Cu, 12.23. IR data [ν/cm^{-1}] on KBr disk: 3025 (aromatic C−H), 2900 (aliphatic C−H), 1590, 1560 (pyridine ring), 1450 (C−H bending), and 770 (pyridine C−H bending). FAB-MS data: *m*/*z* 443 $[M - Br]^+$, 354 $[M - 2Br]^+$, and 290 $[M - Cu - 2Br]^+$.

$[Cu(Br)_2(L1OMe)]$ (10). By mixing L1 (289 mg, 1.0 mmol) with $CuBr_2$ (223 mg, 1.0 mmol) in MeOH (15 mL), **9** was generated as brown precipitate, which was stirred under air for 48 h to give a brown suspension with yellow precipitate. The yellow precipitate was removed by filtration. The filtrate was concentrated to dryness and the residue was recrystallized from CH_2Cl_2/C_6H_6 to give brown crystals of **10** suitable for X-ray structure analysis. **10**: IR data [ν/cm^{-1}] on KBr disk: 3050 (aromatic C−H), 2900 (aliphatic C−H), 1600, 1560, 1510, (pyridine ring), 1450 (C−H bending), 1060, 1040 (ether C−O−C) and 775 (pyridine C−H bending). FAB-MS data: *m*/*z* 464 $[M - Br]^+$, 382 $[M - 2Br]^+$, and 320 $[M - Cu - 2Br]^+$.

Reaction of 9 with Cyclohexene. To a solution of cyclohexene (1 mL) in CH_2Cl_2 (5 mL) were added 5.35 mg **9** and 3.0 μL of nitrobenzene as an internal standard for GLC analysis. The mixture was stirred under air for 1 day, then the brown solid **9** disappeared and yellow solid **5** was generated. After filtration, 4.3 mg (yield 95%) of **5** was obtained. As the sole detectable product *trans*-1,2-dibromocyclohexane was generated from cyclohexene. The yield of the product was determined by GLC analysis to be 98% based on the amount of **9** used.

Oxygenated Products of L1. Reaction of L1 with $CuBr_2$ under Stoichiometric Conditions. In the course of the reaction of L1 (289 mg, 1 mmol) with $CuBr_2$ (223 mg, 1.0 mmol) under the stoichiometric conditions in MeOH (15 mL) under air, an aliquot was taken from the reaction mixture and concentrated to dryness. To the residue were added CH_2Cl_2 and concentrated NH_3, and the mixture was stirred vigorously for 1 h. The aqueous layer turned blue. The CH_2Cl_2 layer was separated from the aqueous layer, washed with distilled H_2O (10 mL × 3), and concentrated to dryness. To the residue was added toluene as an internal standard. The yields of the oxygenated ligands tris(6-methyl-2-pyridyl)-methanol (L1OH), tris(6-methyl-2-pyridyl)methoxymethane (L1OMe), and bis(6-methyl-2-pyridyl) ketone (bpk) were determined by the integral values of the methyl groups of the oxygenated ligands and toluene in the ^{1}H NMR spectrum. Finally, the whole reaction mixture was worked up, and L1OH, L1OMe, and bpk were isolated and purified by silica gel column chromatography. The developing solvent is a mixture of $CHCl_3$ and AcOEt. L1OH: Anal. Calcd for $C_{19}H_{19}N_3O$: C, 74.29; H, 6.27; N, 13.76. Found: C, 74.31; H, 6.31; N, 13.49. IR data [ν/cm^{-1}] on KBr disk: 3200 (O−H), 3050 (aromatic C−H), 2950, 2900 (aliphatic C−H), 1585, 1568 (pyridine ring) 1445 (pyridine C−H bending) 1385 (O−H bending), 1070 (C−O), and 780 (pyridine C−H bending). ^{1}H NMR data (δ/ppm vs Me_4Si in $CDCl_3$): 7.49, (d, 3H, py-3), 7.27 (t, 3H, py-4), 7.00 (d, 3H, py-5), and 2.49 (s, 9H, methyl). FAB-MS data: *m*/*z* 306 $[M]^+$, 288 $[M - OH]^+$, and 213 $[M - Mepy]^+$. L1OMe: Anal. Calcd for $C_{20}H_{21}N_3O$: C, 75.21; H, 6.63; N, 13.16. Found: C, 74.63; H, 6.83; N, 13.05. IR data [ν/cm^{-1}] on KBr disk: 3050 (aromatic C−H), 2950, 2900 (aliphatic C−H), 1585, 1568 (pyridine ring), 1445 (pyridine C−H bending), 1070 (C−O), and 780 (pyridine C−H bending). ^{1}H NMR data (δ/ppm vs Me_4Si in $CDCl_3$): 7.49, (m, 6H, py-3, 5), 7.01 (t, 3H, py-4), 3.29 (s, 3H, methoxy), and 2.48 (s, 9H, methyl). FAB-MS data: *m*/*z* 320 $[M]^+$ and 288 $[M - OMe]^+$. bpk: Anal. Calcd for $C_{13}H_{12}N_2O$: C, 73.57; H, 5.70; N, 13.20. Found: C, 73.53; H, 5.60; N, 13.09. IR data [ν/cm^{-1}] on KBr disk: 3050 (aromatic C−H), 2950, 2900 (aliphatic C−H), 1680 (carbonyl), 1585 (pyridine ring), 1450 (C−H bending), and 1330, 990, 765. ^{1}H NMR data (δ/ppm vs Me_4Si in $CDCl_3$) 7.89, (d, 2H, py-3), 7.74 (t, 2H, py-4), 7.34 (d, 2H, py-5), and 2.63 (s, 6H, methyl). FAB-MS data: *m*/*z* 213 $[M]^+$.

Reaction of L1 with $CuBr_2$ under Catalytic Conditions. The reaction of L1 (289 mg, 1 mmol) with $CuBr_2$ (22.3 mg, 0.1 mmol) was carried out in MeOH (15 mL) under air. The oxygenation of L1 was monitored by ^{1}H NMR spectra of the crude products by taking an aliquot from the reaction mixture during the course of the reaction. The yields of L1OH, L1OMe, and bpk were determined as described above. Finally, the whole reaction mixture was worked up, and L1OH, L1OMe, and bpk were isolated and purified by column chromatography as described above.

Reaction of L1 with the Other Cu(II) Salts. To a solution of L1 (28.9 mg, 0.1 mmol) in MeOH (2 mL) was added a catalytic amount of $Cu(NO_3)_2$, $CuSO_4$, or $Cu(ClO_4)_2$ (L1:Cu(II) salt = 1:0.1, mol/mol) and the mixture was stirred under air. The reaction was followed as described above by ^{1}H NMR spectra. L1OH and bpk were detected as the oxygenated products of L1, but L1OMe was not produced. For $Cu(NO_3)_2$, the yields of L1OH and bpk after 1 day are 39% and 17%, and after 2 days, 71% and 29%, respectively. For $Cu(ClO_4)_2$, the yields of L1OH and bpk after 1 day are 30% and 16%, and after 2 days, 69% and 26%, respectively. For $CuSO_4$, the yields of L1OH and bpk after 1 day are 15% and 9%, and after 2 days, 44% and 20%, respectively.

Reaction of L1 with $Cu(NO_3)_2$ in the Presence of Br_2. To a solution of L1 (28.9 mg, 0.1 mmol) in MeOH (2 mL) were added a catalytic amount of $Cu(NO_3)_2$ (2.0 mg, 0.01 mmol) and a drop of Br_2. The mixture was stirred under air for 1 day. The reaction mixture was worked up and demetalated by treating with concentrated NH_3/CH_2Cl_2 as described above. The oxygenated metal-free ligand was only L1OMe. The yield of L1OMe was 54%.

Reaction of 5 in the Presence of Br_2. To a suspension of **5** (43.3 mg, 0.1 mmol) in MeOH (2 mL) was added a few drops of Br_2, and the mixture was stirred under air. The yellow solid **5** disappeared in 1 day and a green solution appeared, then the reaction mixture was worked up and demetalated by treating with concentrated NH_3/CH_2Cl_2 as described above. The oxygenated metal-free ligand was only L1OMe. The yield of L1OMe was 62%.

Isotope (^{18}O and ^{2}H) Labeling Experiments. [^{18}O]-1. A mixture of $CuBr_2$ (223 mg, 1.0 mmol) and L1 (289 mg, 1.0 mmol) in MeOH (15 mL) was stirred under $^{18}O_2$ for 24 h. To the reaction mixture was added a solution of NaOH (50 mg, 1.25 mmol) in MeOH (5 mL). The stirring under $^{18}O_2$ was continued for 18 h. The ^{18}O-labeled Cu(II)$_3$ complex [^{18}O]-**1** (157 mg, 32%) was isolated as described in the synthesis of **1**. [^{18}O]-**1**: FAB-MS data: *m*/*z* 1340−1325 $[M]^+$, 1195−1180 $[M - PF_6]^+$, and 1115−1100 $[M - Br - PF_6]^+$. IR data [ν/cm^{-1}] on KBr disk: 3050 (aromatic C−H), 2900 (aliphatic C−H), 1600, 1580, 1565, 1450 (pyridine ring), 1075 (C−^{18}O), 840 (PF_6), and 785 (pyridine C−H bending). The metal-free ligand of [^{18}O]-**1** was obtained by treating [^{18}O]-**1** with concentrated NH_3/CH_2Cl_2. FAB-MS data of the metal-free ligand of [^{18}O]-**1**: *m*/*z* 308 and 306 $[M]^+$, 288 $[M - OH]^+$, and 215 and 213 $[M - Mepy]^+$.

Table 1. Crystallographic Data for **1**·C_6H_6, **9**, and **10**

	1·C_6H_6	**9**	**10**
formula	$C_{63}H_{60}N_9O_3P_2F_{12}Cu_3Br$	$C_{19}H_{19}N_3CuBr_2$	$C_{20}H_{21}N_3OCuBr_2$
fw	1551.70	512.73	1551.70
cryst system	cubic	triclinic	triclinic
space group	*I*23 (No. 197)	$P\bar{1}$ (No. 2)	*P*1 (No. 2)
a/Å	24.413(3)	8.515(3)	11.215(4)
b/Å		14.598(5)	11.381(3)
c/Å		8.253(3)	9.538(3)
β/deg			
V/Å^3	14450(4)	962.5(6)	1030.0(6)
Z	8	2	2
T/°C	23	20	20
D_c/g cm^{-3}	1417	1.769	1.756
radiation(λ)/Å	Cu Kα 1.54178	Mo Kα 0.71069	Mo Kα 0.71069
μ/cm^{-1}	27.56	53.05	49.70
R, R_w[a]	0.068, 0.098	0.042, 0.049	0.042, 0.047
GOF index	1.27	1.06	0.85

[a] $R = \Sigma\,||F_o| - |F_c||/\Sigma|F_o|$. $R_w = [\Sigma w(|F_o| - |F_c|)^2/\Sigma w(F_o)^2]^{1/2}$, where $w = 1/\sigma^2(F_o)$.

L1^{18}OH and L1OCD$_3$. A mixture of $CuBr_2$ (22.3 mg, 0.1 mmol) and L1 (289 mg, 1.0 mmol) in CD_3OD (15 mL) was stirred in the absence of NaOH under $^{18}O_2$ for 2 days. The reaction mixture was concentrated to dryness and the residue was treated with concentrated NH_3/CH_2Cl_2 to give a crude mixture of the oxygenated ligands L1^{18}OH, L1OCD$_3$, and bpk. L1^{18}OH (43 mg, 14%), L1OCD$_3$ (97 mg, 30%), and bpk (21 mg, 10%) were isolated and purified by a silica gel column chromatography as described above. L1^{18}OH: FAB-MS data: *m*/*z* 308 [M^{18}O]$^+$, 288 [M^{18}O − ^{18}OH]$^+$, and 215 [M^{18}O − Mepy]$^+$. IR data [ν/cm^{-1}] on KBr disk: 3200 (O−H), 3050 (aromatic C−H), 2950, 2900 (aliphatic C−H), 1585, 1568 (pyridine ring), 1445 (C−H bending), 1385 (O−H bending), 1060 (C−^{18}O), and 780 (aromatic ring). L1OCD$_3$: ^{1}H NMR data (δ/ppm vs Me_4Si in $CDCl_3$): 7.49, (m, 6H, py-3, 5), 7.01 (t, 3H, py-4), and 2.48 (s, 9H, methyl). FAB-MS data: *m*/*z* 323 [M]$^+$and 288 [M − OCD$_3$]$^+$. Spectral data of bpk isolated from the ^{18}O-labeling reaction are exactly the same as those of bpk obtained upon the nonlabeling reaction shown above.

Structure Determination of Single Crystals. The structure of **1**·C_6H_6 was determined on a Rigaku AFC7R diffractometer with graphite monochromated Cu−Kα radiation and a 12 kW rotating anode generator at 296 ± 1 K. The structures of **2**·MeCN·CH_2Cl_2·C_6H_6, **3**, **4**·C_6H_6, **9**, and **10** were determined on a Rigaku AFC7R diffractometer with graphite-monochromated Mo−Kα radiation and a 12 kW rotating anode generator at 293 ± 1 K. Total numbers of reflections, 1671, 4636, 2763, 4511, 7839, and 5027 were collected for **1**·C_6H_6, **2**·MeCN·CH_2Cl_2·C_6H_6, **3**, **4**·C_6H_6, **9**, and **10**, respectively. The intensities of three representative reflections were measured after every 150 reflections. All six structures were solved by the direct methods (SHELEXS 86)[57] and expanded using Fourier techniques. The function minimized was $\Sigma w(|F_o| - |F_c|)^2$ with $w = 1/\sigma^2(F_o)$. The neutral atom scattering factors were taken from Cromer and Waver.[58] Anomalous dispersion effects were included in F_c,[59] the values for $\Delta f'$ and $\Delta f''$ being taken from the ref 60 and those for the mass-attenuation coefficients from ref 61. All calculations were performed using the teXan crystallographic software package.[62] Key facets of the structure determinations for **1**·C_6H_6, **9**, and **10** are given in Table 1.

Results and Discussion

Preparation of L1 and L2. The sterically hindered trispyridylmethane ligands L1 and L2 are prepared by stepwise cross-coupling reactions from 2,6-lutidine and 2-bromo-6-picoline (or 2-bromopyridine) as shown in Scheme 1. The stepwise method gives better yields of L1 and L2 than the one-pot reaction previously adopted to prepare a similar tripyridylmethane ligand, 2-(bis(2-pyridyl)methyl)-6-methylpyridine.[18] For the first reaction of the stepwise reactions, Pd(dppf)Cl_2 is a better catalyst than Pd(PPh_3)$_4$, and the yield of the cross-coupling product is increased in the presence of $ZnCl_2$.[63] On the other hand, for the second reactions, better results are obtained by using Pd(PPh_3)$_4$ instead of Pd(dppf)Cl_2 in the absence of $ZnCl_2$.

Scheme 1

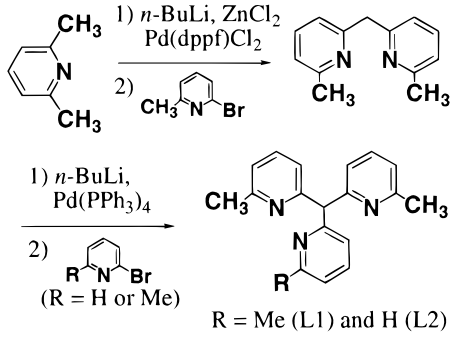

Synthesis of the Cu(II)$_3$ Complexes 1−4. At the beginning of this study, we attempted to synthesize the di-μ-hydroxodicopper(II) complex[63] of L*n*. The reaction of L1 with $CuBr_2$ under the stoichiometric conditions (L1:$CuBr_2$ = 1:1, mol/mol) was carried out in the presence of NaOH, but the di-μ-hydroxodicopper(II) complex was not obtained from the reaction and a green suspension with a yellow solid was obtained. The yellow solid is characterized as a Cu(I) complex $[Cu(L1)Br]_m$ (m = 1 or 2), **5**, which is stable against oxidation under air. L1 may stabilize the Cu(I) state of **5** because tripyridylmethane is known to stabilize low valence states of various metal ions,[8−13] and furthermore, the methyl groups introduced at six positions of the pyridyl groups in L1 as a steric hindrance may enhance the stability of the Cu(I) state of **5**.[65] After addition of NH_4PF_6 to the filtrate, **1** was obtained as a green solid. The FAB MS spectrum of **1** shows major peaks at *m*/*z* 1325, 1246, 1180, and 1040, assignable to $\{[Cu_3(Br)(L1O)_3](PF_6)_2\}^+$, $\{[Cu_3(L1O)_3](PF_6)_2\}^+$, $\{[Cu_3(Br)(L1O)_3](PF_6)\}^+$, and $\{[Cu_3(L1O)_3](PF_6)\}^+$,

(57) Sheldrick, G. M. *Acta Crystallogr. A* **1990**, *46*, 467.
(58) Cromer, D. T.; Waber, J. T. *International Tables for X-ray Crystallography*; Kynoch Press: Birmingham:, 1974; Vol. 4.
(59) Ibers, J. A.; Hamilton, W. C. *Acta Crystllogr.* **1964**, *17*, 781.
(60) Creagh, D. C.; McAuley, W. J. *Internatiuonal Tables for X-ray Crystallography*; Kluwer: Boston: 1992.
(61) Creagh, D. C.; Hubbell, H. H. *Internatiuonal Tables for X-ray Crystallography*; Kluwer: Boston: 1992.
(62) Single-crystal structure analysis software, version 1.6, Molecular Structure Corp., The Woodlands, TX 77381, 1993.
(63) Hayashi, T.; Konishi, M.; Kobori, Y.; Kumada, M.; Higuchi, T.; Hirotsu, K. *J. Am. Chem. Soc.* **1984**, *106*, 158.
(64) Kodera, M.; Simakoshi, H.; Tachi, Y.; Katayama, K.; Kano, K. *Chem. Lett.* **1998**, 441.
(65) Hayashi, Y.; Suzuki, M.; Uehara, A.; Mizutani, Y.; Kitagawa, T. *Chem. Lett.* **1992**, 91.

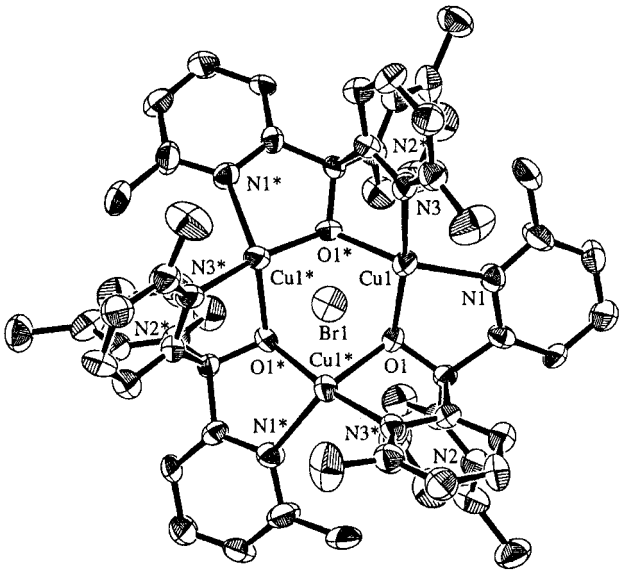

Figure 1. ORTEP view of cationic portion of $[Cu_3(Br)(L1O)_3](PF_6)_2 \cdot C_6H_6$ with the atom numbering scheme (50% probability ellipsoids). Selected bond distances (Å): Cu1−Cu1*, 3.302(3); Cu1−Br1, 2.836(2); Cu1−O1, 1.883(9); Cu1−O1*, 2.001(8); Cu1−N1, 2.059(10); Cu1−N3, 1.97(1). Selected bond angles (deg): Cu1−O1−Cu1*, 116.4(4); O1−Cu1−O1*, 92.9(5); O1−Cu1−N1, 81.9(4); O1−Cu1−N3, 170.7(4); O1*−Cu1−N1, 136.4(4); O1*−Cu1−N3, 82.5(4); N1−Cu−N3, 107.1(4).

respectively, suggesting that **1** has a $Cu(II)_3$ unit, $Cu_3(L1O)_3$. Eventually, the structure of $[Cu_3(Br)(L1O)_3](PF_6)_2$ **1** was revealed by the X-ray structure analysis described below. The yield of **1** is low when $CuBr_2$ and NaOH were added simultaneously to a solution of L1 in MeOH and improved to 37% when NaOH was added to the reaction mixture after the reaction of L1 and $CuBr_2$ for 24 h under the stoichiometric conditions (L1:$CuBr_2$ = 1:1, mol/mol). Furthermore, the yield of **1** is improved to 64% when a catalytic amount of $CuBr_2$ was used (L1:$CuBr_2$ = 1:0.1, mol/mol). The $Cu(II)_3$ complexes **2**−**4** and the Cu(I) complexes **6**−**8** were obtained from the reaction of L*n* (*n* = 1 and 2) with CuX_2 (X = Br and Cl) under similar conditions.

Crystal Structures of 1−4. The ORTEP view of the cation, $[Cu_3(Br)(L1O)_3]^{2+}$, of **1** is shown in Figure 1 together with the numbering scheme. The selected bond distances and bond angles of **1** are shown in the caption of Figure 1. The ORTEP views of **2**−**4** are available as Supporting Information.

The cation of **1** lies on a crystallographic 3-fold axis and, accordingly, has exact 3-fold symmetry. The three Cu atoms of **1** are located at the apexes of an equilateral triangle, and bridged by three μ-alkoxo O atoms of L1O to form a Cu_3O_3 core. The Cu atoms are each coordinated by two pyridyl N atoms, two bridging alkoxo O atoms, and Br atom and assumes a distorted trigonal bipyramidal geometry. Two of three pyridyl groups of L1O bind to different Cu atoms, and the other one is free from coordination. The Br atom of **1** lies on the 3-fold axis, bridges three Cu atoms to form a μ_3-Br bridge, and is surrounded by hydrophobic walls of three coordinated pyridyl groups. The structure of **2** is similar to that of **1**, but the μ_3-bridge of **2** is a chloride ion. The structures of **3** and **4** are similar to those of **1** and **2**, respectively, but the sterically less hindered ligand (L2O) binds to the Cu atom in **3** and **4**. One of two 6-methyl-2-pyridyl groups of L2O is free from coordination in **3** and **4**.

The Cu−N and Cu−O bond distances in **1**−**4** are typical of other Cu(II) complexes. The distances of the Cu−X (X = Br and Cl) bonds of **1**, **2**, **3**, and **4** are 2.836(2), 2.683(9), 2.804(3), and 2.675(3) Å, respectively. These distances are much larger than those of ordinary Cu(II)−X bonds, suggesting that the Cu−X bonds in **1**−**4** are weak. Actually, **1** is easily converted to a Br-free complex $[Cu_3(L1O)_3](PF_6)_2(BF_4)$ when treated with $AgBF_4$. The easy exchange of the μ_3-X bridges is one of the prominent properties of **1**−**4**. The difference of the Cu−X bond distances in **1**−**4** mainly depends on the size of the halide ions. The Cu−Cu distances of **1**, **2**, **3**, and **4**, are 3.302(3), 3.276(5), 3.276(3), and 3.248(2) Å, respectively. The Cu−Cu distances of **1** and **2** are larger by ca. 0.027 Å than those of **3** and **4**, respectively. Since L1O in **1** and **2** is sterically more hindered than L2O in **3** and **4**, this difference may come from the steric repulsion between the LnO ligands. The Cu−Cu distances in **1** and **3**, having a μ_3-Br bridge, are larger by ca. 0.027 Å than those in **2** and **4**, having a μ_3-Cl bridge, respectively. Thus, the Cu−Cu distances in **1**−**4** depend on both the steric hindrance of LnO and the size of the halide ions to a similar extent.

The bond angles of the O(1)−Cu(1)−N(3) and the O(1*)−Cu(1)−N(1) are the largest and the second largest in bond angles around the Cu atom in **1** and are 170.7(4)° and 136.4(4)°, respectively. The τ value[67] calculated from these angles for **1** is 0.57. The τ values calculated for **2**, **3**, and **4** by the same way are 0.60, 0.52, and 0.63, respectively. The τ values vary from 0, for an idealized square pyramid, to 1, for an idealized trigonal bipyramid.[65] The copper coordination geometry in **1**−**4** can be described as a rather distorted trigonal bipyramid.

Many examples have been reported for triangular Cu_3 complexes.[20−32] Most of them have an equilateral triangle of three Cu(II) ions bridged by a mono-μ_3-OH or a mono-μ_3-O with a Cu−Cu distance (3.17−3.38 Å), and their $Cu(II)_3$ cores are supported by three lateral μ-N−O bridges of oximato ligands[20−25] (or μ-N−N bridge of pyrrazolato ligand)[25] and, in a few examples, by three lateral μ-carbonyl oxygen bridges.[28,29] There is an example of a doubly μ_3-OH-bridged $Cu(II)_3$ complex with a Cu−Cu distance of 2.808(3) Å.[31] The double μ_3-OH bridges shorten the Cu−Cu distance. Stack et al. determined the crystal structure of a doubly μ_3-O-bridged Cu_3(II,II,III) complex which is formed from O_2-oxidation of a Cu(I) complex of *N*,*N*,*N*,*N*-tetramethyl-1,2-diaminocyclohexane.[32] The double μ_3-O bridges stabilize the Cu(III) state. The Cu_3-based triangle is isosceles due to the Cu(III) ion to give two Cu−Cu distances, 2.641(3) and 2.705(2) Å, much shorter than the distances in the μ_3-OH-bridged $Cu(II)_3$ complexes. The doubly μ_3-OH- or μ_3-O-bridged Cu_3 complexes do not have the lateral bridge. The μ_3-OH and μ_3-O bridges stabilize the Cu_3 core structure and control the valence state of the Cu ion. The present $Cu(II)_3$ complexes **1**−**4**, however, do not have either μ_3-OH or μ_3-O bridges. Instead, the μ_3-position of **1**−**4** is occupied by a Br or Cl ion, which weakly binds to the Cu atoms. The $Cu(II)_3$ core structures in **1**−**4** are mainly stabilized by the three lateral μ-alkoxo bridges and only weakly supported by the μ_3-X bridge. Therefore, **1**−**4** are structurally quite unique in equilateral triangular $Cu(II)_3$ complexes reported so far.

Magnetic Properties of 1−4. The magnetic susceptibility measurements of **1**−**4** were made on the crystals in the temperature range 4.2−290 K. The temperature dependence of the magnetic susceptibility (χ_M) and effective magnetic moment (μ_{eff}) per molecule of **1** is shown in Figure 2. The temperature

(66) Kodera, M.; Terasako, N.; Kita, T.; Tachi, Y.; Kano, K.; Yamazaki, M.; Koikawa, M.; Tokii, T. *Inorg. Chem.* **1997**, *36*, 3861.
(67) Addison, A. W.; Rao, T. N.; Reedijk, J.; Rijin, J. V.; Verschoor, G. C. *J. Chem. Soc., Dalton Trans.* **1984**, 1349.

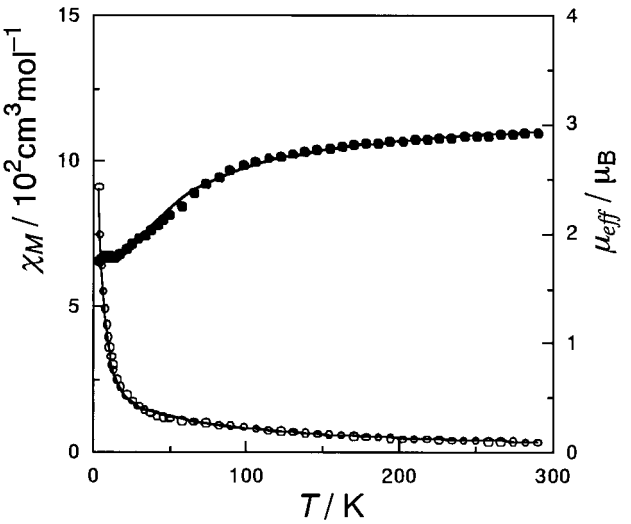

Figure 2. Temperature dependence of χ_M (○) and μ_{eff} (●) of **1**·C_6H_6. Solid curves are based on eq 1, using $J = -19.5$ cm^{-1}, $g = 2.02$, and $N\alpha = 60$.

Table 2. Magnetic Susceptibility Parameters

compound	J/cm^{-1}	g	$N\alpha$
1·C_6H_6	−19.5	2.02	60
2·MeCN·CH_2Cl_2·C_6H_6	−3.70	2.01	60
3	−4.80	2.00	60
4·C_6H_6	−0.30	2.01	60

dependence of χ_M and μ_{eff} in the temperature range from 4.2 to 290 K for **2**−**4** are available as Supporting Information.

As the temperature is lowered, the μ_{eff} per molecule of **1** decreases from 2.95 at 290 K to 1.75 at 4.2 K, indicating that an antiferromagnetic interaction operates among the three Cu(II) ions. When three paramagnetic metal ions of $S = {}^1/_2$ are equivalent and form an equilateral triangle, the magnetic exchange interaction may be described by the single parameter J. The temperature dependence of χ_M for **1**−**4** is simulated by the equation shown below:[25]

$$\chi_M = (Ng^2\beta^2/4kT)[5 + \exp(-3J/kT)] \times [1 + \exp(-3J/kT)]^{-1} + N\alpha \quad (1)$$

An excellent fit of the $\chi_M - T$ data to the simulation was obtained when $J = -19.5$ cm^{-1}, $g = 2.02$, and $N\alpha = 60$ were assumed for **1**. The best fitting parameters for **1**−**4** are summarized in Table 2.

The isotropic exchange interaction among three ions of $S = {}^1/_2$ placed at the apexes of an equilateral triangle splits the three degenerate energy levels into one quartet state with a total spin $S_T = {}^3/_2$ and two degenerate doublet states with $S_T = {}^1/_2$. The separation energy between the $S_T = {}^3/_2$ and $S_T = {}^1/_2$ states is 58.5 cm^{-1} ($-3J$) for **1**. The μ_{eff} value, 1.75 μ_B, of **1** per molecule at 4.2 K indicates that the ground doublet states are occupied predominantly and the spin of the tricopper unit is close to ${}^1/_2$. On the other hand, the μ_{eff} values at 4.2 K for **2**, **3**, and **4** are 1.95, 1.93, and 2.80 μ_B, respectively, larger than 1.73 μ_B of the spin only value for $S = {}^1/_2$. In **4**, the μ_{eff} values are almost constant at temperatures between 4.2 and 290 K, indicating that the magnetic interaction between the Cu(II) ions is very weak and the excited quartet state is considerably populated even at 4.2 K.

The J values, −0.30 to −4.8 cm^{-1}, found for **2**−**4** are much lower than the values reported for the mono-μ_3-OH(or O)-bridged Cu(II)$_3$ complexes with oximato (−122 to −1000 cm^{-1})[20−25] or pyrrazolato (−200 cm^{-1})[27] ligands and slightly lower than the values (−12 and −15 cm^{-1})[28,29] reported for the mono-μ_3-OH-bridged Cu(II)$_3$ complexes with the μ-carbonyl oxygen bridges. The three Cu(II) ions in the μ_3-OH(or O)-bridged complexes are magnetically coupled to each other by a superexchange interaction through the μ_3-OH (or O) bridge. The strong magnetic interaction for the oximato- and pyrrazolato-bridged complexes is owing to the effective overlap of the magnetic orbitals ($d_{x^2-y^2}$) because of the coplanarity of the coordination planes of the three subunits.[25,27] On the other hand, the relatively weak magnetic interaction for the Cu(II)$_3$ complexes bridged by μ-carbonyl oxygen is due to orthogonality of the three magnetic orbitals ($d_{x^2-y^2}$) which are directed to the μ_3-OH bridge.[29] The coordination geometry about each copper atom in **1**−**4** is nearly trigonal bipyramidal, which leads to a dz^2 ground state. The three major lobes of the dz^2 orbitals (magnetic orbitals) are oriented along three alternate sides in a hexagon of the Cu_3O_3 core in **1**−**4** and cannot overlap each other. This leads to the very weak magnetic interaction between the Cu(II) ions in **1**−**4**.

The 4.2 K EPR spectrum of **1**, however, shows a feature of a hyperfine structure due to the parallel component with $g_{parallel} = 2.25$, which is larger than $g_{perpendicular}$. This is indicative of a $d_{x^2-y^2}$ electronic ground state, showing that the coordination geometry of the Cu atom in **1**−**4** in solution is square pyramidal. The hyperfine splitting of the parallel component is a complicated multiplet and broadened due to a spin delocalization between the three Cu atoms. The EPR spectra of **2**−**4**, at 4.2 K, are similar to that of **1**, but the hyperfine splittings of the parallel components of **2**−**4** are much more complicated. This may be explained by contribution of the quartet state of the Cu(II)$_3$ unit due to the weaker antiferromagnetic interaction of **2**−**4** compared with **1**. The EPR spectra of **1**−**4** are available as Supporting Information.

Formation of 9 and 10. [Cu(Br)$_2$(L1)] (**9**) is formed by the reaction of L1 with $CuBr_2$ under anaerobic conditions. Just after mixing L1 with $CuBr_2$ in MeOH, **9** precipitated as a brown solid. The yield of **9** is quantitative. [Cu(Br)$_2$(L1OMe)] (**10**) is formed by stirring **9** in MeOH under air. The structures of **9** and **10** were determined by X-ray analyses. The ORTEP view of **9** is shown in Figure 3. The Cu atom in **9** is coordinated to three pyridyl N atoms of L1 and two Br atoms to create a distorted square pyramidal geometry. The structure of **9** shows that L1 is unmodified in the first step of the reaction of L1 with $CuBr_2$. The oxygenation of L1 must proceed via **9** by considering the quantitative yield of **9**. The ORTEP view of **10** is shown in Figure 4. The structure of **10** reveals that the methine carbon of L1 is substituted by a methoxy group to form tris(6-methyl-2-pyridyl)methoxymethane (L1OMe). The Cu atom in **10** is coordinated to two pyridyl N atoms and an O atom of L1OMe and two Br atoms to create a distorted square pyramidal geometry. These structures of **9** and **10** clearly demonstrate that L1 is converted to L1OMe in the reaction of L1 with $CuBr_2$ in MeOH under air.

When **9** was converted to **5** in the presence of cyclohexene, *trans*-1,2-dibromocyclohexane was obtained quantitatively but not *cis*-1,2-dibromocyclohexane, indicating that cyclohexene is brominated by Br_2 generated in the reaction system. The driving force to generate Br_2 may be owing to the high stability of **5**. It seems that the Br_2 generated plays an important role in the oxygenation of L1.

Oxygenated Products of L1. During the reaction of L1 with $CuBr_2$ in MeOH under air, an aliquot was taken from the reaction mixture, concentrated, and treated with concentrated

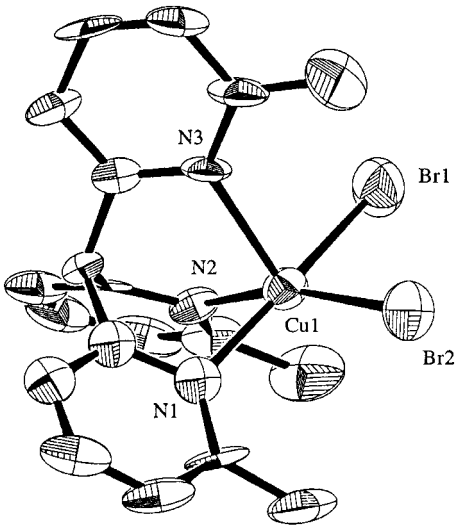

Figure 3. ORTEP view of $[CuBr_2(L1)]$ (**9**) with the atom numbering scheme (50% probability ellipsoids). Selected bond distances (Å): Cu−Br1, 2.398(2); Cu1−Br2, 2.455(3); Cu1−N1, 2.10(1); Cu1−N2, 2.02(1); Cu1−N3, 2.33(1). Selected bond angles (deg): Br1−Cu1−Br2, 93.06(9); Br1−Cu1−N1, 93.3(3); Br1−Cu1−N2, 163.4(3); Br1−Cu1−N3, 101.3(3); Br2−Cu1−N1, 172.6(3); Br2−Cu1−N2, 91.3(3); Br2−Cu1−N3, 92.1(3); N1−Cu1−N2, 81.5(4); N1−Cu1−N3, 90.2(4); N2−Cu1−N3, 94.6(4).

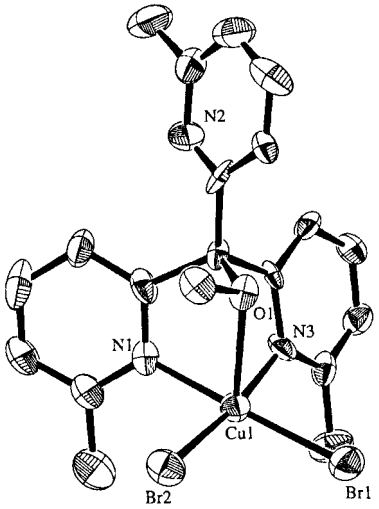

Figure 4. ORTEP view of $[Cu(Br)_2(L1OMe)]$ **10** with the atom numbering scheme (50% probability ellipsoids). Selected bond distances (Å): Cu1−Br1, 2.378(2); Cu1−Br2, 2.405(2); Cu1−O1, 2.382(7); Cu1−N1, 2.049(9); Cu1−N3, 2.037(9). Selected bond angles (deg): Br1−Cu1−Br2, 93.61(7); Br1−Cu1−O1, 102.5(2); Br1−Cu1−N1, 174.7(2); Br1−Cu1−N3, 94.3(2); Br2−Cu1−O1, 98.8(2); Br2−Cu1−N1, 91.5(2); Br2−Cu1−N3, 171.7(3); O1−Cu1−N1, 78.1(3); O1−Cu1−N3, 77.0(3); N1−Cu1−N3, 80.6(3).

NH_3/CH_2Cl_2. A crude mixture of the oxygenated metal-free ligands L1OH, bpk, and L1OMe was obtained from the CH_2Cl_2 extracts. When $CuCl_2$ was used instead of $CuBr_2$, the same products were obtained. The transformation of L1 in the reaction with $CuBr_2$ in MeOH under air and in the treatment with NaOH is shown in Scheme 2.

The reaction is followed by ^{1}H NMR spectra of the crude mixture of the oxygenated metal-free ligands. The yields of L1OH, bpk, and L1OMe for 1 day of reaction under the stoichiometric conditions are 10, 4, and 27%, respectively. After the reaction is continued for 2 days, these are increased to 18, 5, and 34%, respectively. In the stoichiometric reaction, it takes more than 1 week to complete the oxygenation of L1. Under

Scheme 2

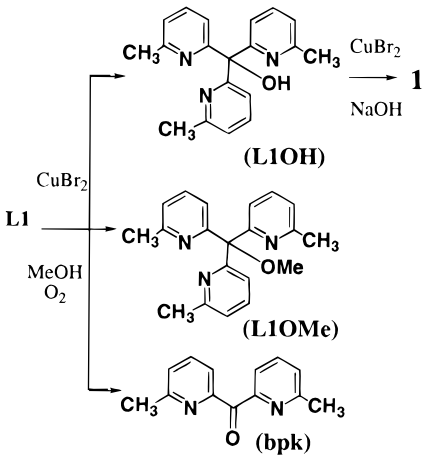

the catalytic conditions, the yields of L1OH, bpk, and L1OMe for 1 day of reaction are 24, 17, and 52%, respectively, and the reaction is complete in 2 days. Both in the stoichiometric and catalytic reactions, the major product is L1OMe. The catalytic reaction is more efficient than the stoichiometric one. This is also found in the Cu-mediated ligand ketonization.[53] In the catalytic reaction, the metal-free L1 is oxygenated, but in the stoichiometric reaction, L1 of **5** is oxygenated. The conformational freedom of the pyridyl groups in L1 of **5** is restricted by the coordinated Cu(I) ion. If the oxygenation of L1 proceeds via a radical intermediate at the methine carbon, the Cu(I) ion prevents the methine carbon in L1 of **5** from taking the planar configuration required for the radical intermediate. This may be one reason the stoichiometric reaction is less efficient than the catalytic reaction.

The oxygenation of L1 is also catalyzed by $Cu(NO_3)_2$, $Cu(ClO_4)_2$, and $CuSO_4$ (L1:Cu salt = 1:0.1, mol/mol) in MeOH under air to give L1OH and bpk, but not L1OMe. The order of efficiency in the oxygenation of L1 is $CuBr_2 \gg Cu(NO_3)_2 > Cu(ClO_4)_2 > CuSO_4$. Since L1OH and bpk were obtained by using any Cu(II) salt, an autoxidation of L1 catalyzed by a Cu(II) ion under air may be proposed as a reaction pathway for the formation of L1OH and bpk. On the other hand, since L1OMe was obtained only by using the Cu(II) halide salts, another reaction pathway must exist for the formation of L1OMe. When the reaction of L1 with a catalytic amount of $Cu(NO_3)_2$ in MeOH under air was carried out in the presence of a drop of Br_2, L1OMe was detected as a major product. When a few drops of Br_2 were added to a suspension of **5** in MeOH, **5** was converted to **10**. L1OMe was also obtained from reaction of L1 with Br_2 without any Cu salt in MeOH under air. These results indicate that Br_2 is essential for the formation of L1OMe.

Isotope-Labeling of the Oxygenated Ligands. The FAB MS spectrum of the ^{18}O-labeled Cu(II)$_3$ complex [^{18}O]-**1** prepared under $^{18}O_2$ shows parent peaks between *m*/*z* 1325 and 1345 due to $\{[Cu_3(Br)(L1O)_3](PF_6)_2\}^+$, indicating that the origin of O atom in L1OH is O_2. To know the origin of the oxygen atom of L1OH and L1OMe, the reaction of L1 with $CuBr_2$ was carried out in CD_3OD under $^{18}O_2$. The oxygenated products of L1 isolated from this reaction were L1^{18}OH, bpk, and L1OCD$_3$ on the basis of all spectral data including FAB MS spectra. L1^{18}OH and L1OCD$_3$ clearly demonstrate that $^{18}O_2$ is incorporated into L1^{18}OH and CD_3OD into L1OCD$_3$. The two different origins of O atoms for L1OH and L1OMe clearly show that two different reaction pathways exist for the oxygenation of L1.

Scheme 3

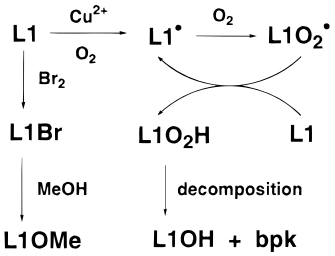

Proposed Mechanism of the Oxygenation of L1. A proposed mechanism for the oxygenation of L1 to L1OH, bpk, and L1OMe is shown in Scheme 3. Two different reaction pathways exist in the oxygenation of L1 with $CuBr_2$ in MeOH under air. One is for the formation of L1OH and bpk and another is for the formation of L1OMe. The formation of L1OH and bpk may be explained by an autoxidation catalyzed by a Cu(II) ion on the basis of the following two pieces of evidences: (1) L1OH and bpk are produced by using any Cu(II) salt under air and (2) the origin of O atom in L1OH is O_2. The mechanism of the autoxidation of L1 is proposed as follows. Initially, L1 is oxidized to a radical (L1$^\bullet$) at the methine carbon in the presence of a Cu(II) ion under air. L1$^\bullet$ reacts with O_2 to form L1$O_2^\bullet$, which abstracts H$^\bullet$ from L1 to give L1O_2H and L1$^\bullet$. L1O_2H decomposes to L1OH and bpk. The facts that (1) Br_2 is essential for the formation of L1OMe and (2) the origin of O atom of L1OMe is MeOH suggest the following reaction pathway for the formation of L1OMe. L1 is brominated at the methine carbon by Br_2, generated when **9** is converted to **5**, to form L1Br, methanolysis of which affords L1OMe.

The ketonization of ligand has been well-studied and is a kind of autoxidation.[50,51] The first step of the ketonization may be one electron (1-e) oxidation of ligand by a metal ion under air. This reaction is accelerated in the presence of a base (OH^- and amines), indicating that the 1-e oxidation is coupled with a proton trap by the base. The second step is oxygenation of the resultant carbon radical (L$^\bullet$) by O_2, which forms alkylhydroperoxide intermediate. The oxygenation of L1 to L1OH and bpk may be similar to the ketonization because both these reactions are catalyzed by various Cu(II) salts and proceed via formation of alkylhydroperoxide intermediate. The methine carbon of L1 and the methylene carbon substituted by two aromatic amines, such as pyridyl, benzimidazolyl, and imidazolyl derivatives, may be easily oxidized to the carbon radicals because they must be stabilized by π-conjugation with the aromatic groups. However, for the formation of L1OMe, the reaction proceeds via the bromination of the methine carbon by Br_2 and the methanolysis of L1Br. Thus, the formation of L1OMe is totally different from the ketonization.

Conclusion

Newly designed sterically hindered trispyridylmethane ligands L1 and L2 are synthesized. The reaction of Ln (n = 1 and 2) with CuX_2 (X = Br and Cl) formed unique equilateral triangular $Cu(II)_3$ complexes **1**−**4**, on the contrary to the expectation that Ln would form di-μ-hydroxodicopper(II) complexes. Compounds **1**−**4** are quite unique in that they do not have neither μ_3-hydroxo or μ_3-oxo bridges and very weak antiferromagnetic interactions operate between the three Cu(II) ions. In the course of the reaction of L1 with $CuBr_2$ in MeOH under air, the oxygenated metal-free ligands L1OH, bpk, and L1OMe were detected. Since this reaction is quite unique, various studies including the isotope labeling with $^{18}O_2$ and CD_3OD were carried out to clarify the mechanism. The oxygenation of L1 with $CuBr_2$ in MeOH under air proceeds through the two different reaction pathways. In one of them, L1OH and bpk are produced via a kind of autoxidation similar to the ketonization. Another one is the formation of L1OMe, and the mechanism might be explained by the methanolysis of L1Br generated from bromination of L1 with Br_2.

Acknowledgment. This work was supported by a Grant-in-Aid for Scientific Research on Priority Areas (No. 10149101 "Metal-assembled Complexes") and a Grant to RCAST at Doshisha University from the Ministry of Education, Science, Sports, and Culture, Japan.

Supporting Information Available: X-ray crystallographic files in CIF format for **1**·C_6H_6, **2**·MeCN·CH_2Cl_2·C_6H_6, **3**, **4**·C_6H_6, **9**, and **10**; ORTEP diagrams of **2**−**4**, figures for temperature dependence of χ_M and μ_{eff} in the temperature range from 4.2 to 290 K for **2**−**4**, and ESR spectra at 4.2 K for **1**−**4**. This material is available free of charge via the Internet at http://pubs.acs.org.

IC990331G